SPACE SCIENCES LABORATORY

Final Report

Radiation Measurement Experiment for Applications Technology Satellite-E

Contract No.: NAS 5-10362

Principal Investigator: Professor F. Mozer

Series 13, Issue 23

March 9, 1972

UNIVERSITY OF CALIFORNIA, BERKELEY

Space Sciences Laboratory Series 13, Issue 23

Final Report

for

RADIATION MEASUREMENT EXPERIMENT FOR APPLICATIONS TECHNOLOGY SATELLITE-E

Contract No.: NAS 5-10362

Goddard Space Flight Center

Contracting Officer: Kent Cockerham
Technical Monitor: Forest Wainscott

Prepared by

Space Sciences Laboratory
University of California
Berkeley, California 94720

Principal Investigator: Professor Forrest Mozer

for

Goddard Space Flight Center
Greenbelt, Maryland 20771

March 9, 1972

LIST OF ILLUSTRATIONS

I. SUMMARY

The ATS-5 satellite was launched on August 12, 1969. To date, the University of California, Berkeley experiment (NASA designation 3DME) has completed nearly 900 days of successful operation. One of the three detectors has been inoperable since launch because of the failure of a mechanical sun-shutter over the entrance aperture. Recent quick-look data indicate that except for the sun-shutter problem, the experiment performance is undegraded.

The first year of data has been fully reduced and selective reduction (during interesting intervals) has been performed on the remaining data. Current data from the experiment are received at Berkeley after a short time delay and are of excellent quality.

Completed studies utilizing the data have been made on a series of topics. These studies are listed in the Bibliography and one copy has been sent to the GSFC library. Data analysis is in progress (budget permitting) on a number of other topics, including bounce-period particle variations, substorm phenomenology, proton injection, etc.

Data have been shared with a number of other experimenters, for the purpose of comparison with their own results from balloon, rocket and satellite experiments. The Berkeley group flew several balloons from the northern terminus of the ATS-5 magnetic field line at Thompson, Manitoba, Canada in 1970. The results from these flights are also given in the Bibliography. The continued operation of the 3DME experiment has prompted the planning of another series of balloon flights from Thompson, scheduled for August, 1972. Measurements will be made of the ionospheric electric field and of

auroral x-ray pulsations; these observations will be compared with the particle fluxes recorded at the synchronous orbit on ATS-5.

The Berkeley experimenters have received excellent cooperation from all NASA personnel associated with the ATS project, which is greatly appreciated.

II. OPERATION OF THE INSTRUMENT

A. Scintillation Detectors

In order to use a single detector for the simultaneous analysis of both protons and electrons, it was decided to use a scintillator of the configuration shown in Figure 1a (Mozer *et al.*, 1968). The 15,000 Å vacuum-vapor-deposited layer of thallium activated cesium iodide stops electrons of energy ≤ 25 keV and protons of energy ≤ 300 keV. Particles of energy higher than these stop in the plastic (NE 102) layer. In addition, alpha particles of energy ≤ 1 MeV lose their energy in the CsI(Tl) layer. The energy loss characteristics of such a scintillator are shown in Figure 1b. Vapor depositions of other materials than CsI(Tl) were attempted [such as NaI(Tl) and CsI(Na)], but only the CsI(Tl) evaporations produced satisfying results. Apparently the other materials required annealling after evaporation; however, this could not be accomplished because of the low melting temperature of the plastic substrate. To prevent warping during the evaporation process, the plastic discs were mounted in a copper holder through which cold water was circulated at all times. An oil-free vacuum system operating at a pressure of less than 10^{-8} torr was used and a system of moveable lids was used over the evaporation boats to ensure complete controllability of the deposition. A quartz oscillator was used to continuously monitor the deposited thickness. The thin, 1000 Å layer of aluminum evaporated on top of the scintillator acts as a light shield to starlight. It was made pinholefree by gentle brushing with a camel's hair brush immediately after evaporation.

Figure 2a shows a photograph of pulses from the anode of the photomultiplier tube taken while the detector observed a beam of 20 keV electrons. Note the 0.7 μsec rise time which is characteristic of the light decay time in CsI(Tl). (The 4 μ sec pulse decay time is induced by the amplifier electronics.) Figure 2b similarly shows the result of a 30 keV electron beam, with the pulse rise time now $\sim$ 7 nsec (not observable on this time scale) which is the light decay time in NE 102. The detector responses to inputs of 60 keV electrons and 60 keV protons are given in Figures 2c and 2d, respectively.

The light output of the vapor-deposited CsI(Tl) layer was compared with that for bulk crystal CsI(Tl) for both electron and proton beams with the result that the scintillation efficiency (in terms of light input to the photomultiplier tube) of the evaporated layers was virtually identical to that of the bulk material (Figure 3a) until the addition of the aluminum layer, after which it dropped by approximately 50% (Figure 3b). Gold light shields were substituted for the aluminum ones with similar results. The cause of this result is still unknown but identical problems have occurred in other experiments (personal communications to the author at the 1968 Scintillation and Semiconductor Symposium). The effect of the aluminum layer on the efficiency of the proton-detecting

CsI(Tl) layer was undesirable but could not be avoided since the light shield was essential.

The above-described scintillators were used in conjunction with RCA C70102M $\frac{3}{4}$-inch photomultiplier tubes especially selected for their low dark current. All tubes were vibration tested and mounted in shock-resistent, molded fiberglass forms, with machined aluminum and plastic collimators.

B. Electronics

Figure 4 presents a slightly simplified block diagram of the electronics associated with one detector. Complete systems and circuit diagrams and all other details are available in the Experimenters Handbook (Westinghouse Defense and Space Center, 1970). Construction of the circuit components was by the welded module technique. Related units were installed on epoxy motherboards with interconnections and power distribution done by #32 magnet wire.

In Figure 4 the output of the photomultiplier tube is fed through a charge-sensitive preamplifier and a fast pulse amplifier in series. The signals are routed by shielded cable. Considerable care was taken with the grounding of the shields in order to avoid ringing. The actual separation of electrons and protons (and alphas) is accomplished by the use of a delay line (Figure 5) passing only pulses of rise-time less than 50 nsec. Thus, only pulses originating in the plastic layer are able to reach the input of the "FAST" threshold discriminators. Pulses from both scintillating layers reach the "SLOW" threshold discriminator inputs, however. Pulses large enough to trigger the threshold discriminators (whose trigger levels vary from channel to channel and are set by the lab-set resistor R2 as shown in Figure 6) produce standardized square voltage pulses at the inputs to the coincidence/anticoincidence gates. When these gates are set in the coincidence mode only the simultaneous arrival of pulses from the "SLOW" and "FAST" threshold discriminators will produce an output pulse to the zener-diode based log count rate meters. The coincidence mode, then, corresponds to plastic pulses, or electrons of energy $\geqslant$25 keV. Similarly, in the anticoincidence mode, the gates respond only to the arrival of "SLOW" pulses unaccompanied by "FAST" pulses. An output in the anticoincidence mode is equivalent to protons of energy less than $\sim$300 keV. (Assuming proper adjustment of the threshold levels.) The final calibration of the instrument and the resulting responses of the various channels to protons and electrons are described in Appendix A, where typical "center" energies are derived for each channel. These typical energies are the ones referred to throughout this paper.

From Figure 4 we see that channel 4 is permanently set in the anticoincidence mode and that it has no log count rate meter. This channel is reserved for counting alpha particles of energy greater than the highest energy protons counted. Those alphas counted are restricted to those stopping in the CsI(Tl) layer. The expected count rate was so low that telemetry was to be digital only, with no analog output, whereas the three electron and proton channels are telemetered in both analog and digital modes.

In addition to the measurements described above, the current supplied to the tenth dynode of the photomultiplier tube was measured. This current provides a measurement of the total light created in the scintillator, and can be interpreted as the total energy incident on the scintillator. This output is referred to as channel 0 and is telemetered as an analog quantity only.

As an example of the results obtained, Figure 7 presents the south detector particle data from all channels for the day of November 9, 1969. The flux values shown result from the instrument calibration.

Other features shown in Figure 4 are a temperature measurement and the light-diode inflight calibration system. A thermistor mounted on the scintillator housing provides a reading on the temperature there. This is necessary because extremes of temperature will affect the light amplitude from the scintillator. The light diode system is used four times each day and provides light pulses of known amplitude from a gallium phosphide light-emitting diode to check on the PM tube gain. This gain will drift with time and can be corrected to the nominal value by means of the commandable high voltage system. The light diodes were extensively tested on the ground for amplitude drift, which was found to be much less than 10% over the expected instrument lifetime.

C. Experiment Sequencing and Telemetry

Both the internal logic system of the experiment (Experimenters Handbook) and the satellite encoder logic system use a hexadecimal system built upon a basic sequence 5.12 seconds in length. Each sequence consists of 16 frames, each of which is subdivided into 16 channels. During those channels in which 3 DME analog data is read out, the data is integrated for the first 10 msec and read out for the last 10 msec of the 20 msec length of the channel. Table 1 presents the telemetry format for one sequence, showing the location of the 3 DME data. The precise order of telemetered 3 DME analog quantities depends on which of 12 commandable readout modes the experiment is in at the time. Table 2 lists the readout order as a function of mode and channel. Note that frames 4, 8 and 12 are always read out in the same order, independent of the readout mode, with proton (anticoincidence) data being telemetered in frames 4 and 12, and electron (coincidence) data being telemetered in frame 8. This override mode enables the examination of each of the experiment's analog quantities at least once per sequence.

The housekeeping data shown in Table 1 consist of the temperature readings from each of the three thermistors and several voltage monitors from the power supply.

One digital data point is read out each sequence, within a 16-sequence format. The arrangement of digital data as a function of sequence (0-15) is given in Table 3 for both

TABLE 1

3 DME TELEMETRY FORMAT IN
ONE 5.12 SECOND SEQUENCE

CHANNEL

FRAME	0	1	2	3	4	5	6	7	8	9	10	11	12	13	14	15
0					← ANALOG DATA →											
1					← ANALOG DATA →											
2					← ANALOG DATA →											
3								← HOUSEKEEPING (HK) →								
4					← ANALOG DATA PROTON OVERRIDE →											
5					← ANALOG DATA →											
6					← ANALOG DATA →											
7																
8					← ANALOG DATA ELECTRON OVERRIDE →											
9					← ANALOG DATA →											
10					← ANALOG DATA →											
11																
12					← ANALOG DATA PROTON OVERRIDE →											
13					← ANALOG DATA →											
14					← ANALOG DATA →											
15									← HK →		DIGITAL →					

→| |← 20 msec.

TABLE 2

3 DME TELEMETRY FORMAT AS A FUNCTION OF READOUT MODE

MODE	SEQUENCE 10 DIGITAL IDENT.		TELEMETRY FORMAT READOUT ORDER											
	COIN	ANTI-COIN	CH 4	CH 5	CH 6	CH 7	CH 8	CH 9	CH 10	CH 11	CH 12	CH 13	CH 14	CH 15
0	18	2	S3	S2	S3	S2	S3	S2	S3	S2	S3	S2	S3	S2
1	19	3	E3	E2	E3	E2	E3	E2	E3	E2	E3	E2	E3	E2
2	21	5	N3	N2	N1l	N0	N3	N2	N1	N3	N2	N1	N0	N3
3	25	9	E3	E2	E1	E0	E3	E2	E1	E3	E2	E1	E0	E3
4	24	8	N2	S2	N2	S2	N2	S2	N2	S2	N2	S2	N2	S2
5	22	6	N2	E2	N2	E2	N2	E2	N2	E2	N2	E2	N2	E2
6	26	10	N1	S3	N2	S2	N3	S1	N1	S3	N2	S2	N3	S1
7	27	11	N1	E1	N2	E2	N3	E3	N1	E1	N2	E2	N3	E3
8	29	13	E2	S3	N2	S2	N3	E3	E2	S3	N2	S2	N3	E3
9	33	17	N1	S1	E1	N2	S2	E2	N3	S3	E3	N0	S0	E0
10	32	16	N2	S2	E2	N2	S2	E2	N2	S2	E2	N2	S2	E2
11	30	14	N2	N2	N2	N2	N2	N2	N2	N2	N2	N2	N2	N2
FRAMES 4, 8, 12 OVERRIDE			N0	S0	E0	N1	S1	E1	N2	S2	E2	N3	S3	E3

TABLE 3

3 DME DIGITAL DATA FORMAT

	NORMAL SEQUENCES	CALIBRATION SEQUENCES	
SEQ.	DIGITAL DATA	DIGITAL DATA	CALIB. SOURCE
0	N3	N3 COINCIDENCE	RADIOACTIVE
1	N2	N2 "	SOURCE
2	E3	E3 "	
3	E2	E2 "	
4	S3	S3 "	
5	S2	S2 "	
6	18	27	50 KHz #1
7	NORTH GAIN	NORTH GAIN	LIGHT #2
8	EAST GAIN	EAST GAIN	DIODE #3
9	SOUTH GAIN	SOUTH GAIN	PULSES #4
10	MODE IDENT.	MODE IDENT.	#4
11	SYNCH. I. D. = 11	SYNCH. I. D. = 11	#4
12	N4	N4	1 KHz #5
13	E4	E4	LIGHT #5
14	S4	S4	DIODE #5
15	S1	S1	PULSES #5
CAL ONLY 16		100 KHz. OSC.	#5
CAL ONLY 17		25	#5

normal sequencing and for the calibration sequencing (18 sequences long) which takes place every 16^3 sequences (approximately 5.8 hours). One sees that sequences 12, 13 and 14 are the only places alpha particle data is read out, so a total of $16 \times 5.12 = 81.92$ seconds passes between consecutive alpha measurements from each detector.

The inflight calibration system is turned on by the spacecraft encoders every 16^3 sequences. During the first six sequences in the calibration mode the experiment amplifiers switch into a low gain mode and count pulses from a Po^{208} radioactive source between the scintillator (several pulses from which are shown in Figure 8a. These counts are sent out in frames 0-5 by the telemetry. For the following three sequences the light diode drivers (schematic shown in Figure 9) put out three pulses (a different amplitude for each sequence) with pulse rise times of 1 msec. During the next three sequences (9-11) the light diode pulses are of fast (5 nsec) rise time with the same amplitude pulses in all three sequences. For sequences 6-11 the amplifier is in the high gain mode and the light diode pulse rate is 50 kHz. For the last six sequences of the calibration the amplifier switches back to low gain and the light diode driver puts out slow (1 msec) pulses at a 1 kHz rate. Figures 8b-d show photos of representative light-diode pulses from sequences 6-8 (50 kHz, slow), 9-11 (50 kHz, fast) and 12-17 (1 kHz, slow), respectively. Comparison of pre-launch calibration-mode data with inflight calibration data enables adjustment of the photomultiplier tube gain to the nominal value.

The calibration mode may also be activated by ground command if desired. Other available ground commands are:

Coincidence/Anticoincidence Command. This decides whether the instrument measures protons or electrons. Frames 4, 8 and 12 are not affected.

Readout Mode Command. The command sets the readout modes to one of those described in Table 2.

Gain Change Commands. One for each detector. Enables adjustment of the PM tube voltage to put the detector in the proper gain state as determined from the inflight calibration system. There are 32 different steps.

III. FORMAT OF TAPES SUBMITTED TO THE NATIONAL SPACE SCIENCE DATA CENTER (NSSDC)

ATSE - 3DME INTERMEDIATE TAPES

0. <u>General</u>

0.1 ½" IBM 729 compatible

0.2 Odd Parity (Binary mode)

0.3 800 bits per inch

0.4 Prepared from Goddard Space Flight Center 3DME tapes

0.5 File Structure

0.5.1 Two record tape identification file

0.5.2 Not more than 50 data files each starting with an identification record. Each data record contains six logical records (logical record = one 5.12 sec sequence). Data files are obtained from Goddard Space Flight Center (called Goddard hereafter) 3DME files, which generally represent about one hour of data each.

0.6 Record Sizes. Tapes are written on a 60 bit machine. "Word" here = 60 bits, 10 characters.

0.6.1 Tape identification record,
= 6 words, 6 × 60 bits, 60 "characters"

0.6.2 Data file times and index record,
= 150 words, 150 × 60 bits, 1500 "characters"

0.6.3 Data file ID records,
= 11 words, 11 × 60 bits, 110 characters

0.6.4 Data records, physical,
= 486 words, 486 × 60 bits, 4860 characters.
Logical records, six to a physical record, contain 81 words.

0.7 Each file ends in an End-of-file (E.O.F.) mark. The tape ends in a double end of file mark (empty file) with no special trailer record.

0.8 These tapes were written on a CDC 6600 machine at the Lawrence Radiation Laboratory, Berkeley, California circa 1970. This document describes the complete structure of the tapes -- there are no hidden system oriented codes or pointers.

1.0 Tape Leader File of 2 Records

1.1 ID record

Word 1	Year (eg 1970)	,	Integer
2	Month (1-12)	,	"
3	Day	,	"
4	Group No.	,	"
5	b3bDMEbbbb	,	CDC Display Code
6	10 character reel identifier		"

1.2 File Times and index record

Word (i, 1) $86400000 \times$ day of year + milliseconds of day of first 5.12 sec

(i, 2) $86400000 \times$ day of year + milliseconds of day of last 5.12 sec

(i, 3) Lawrence Radiation Laboratory, Berkeley CDC System (Sept 1970) disk index to obtain random access to 1st record of file i. Caution: Do not use this index to access records of tapes sent to National Space Science Data Center as some of these tapes have deleted records.

1.2.1 i = 1, 50. Unused cells = 0. Index in (i, 3) is never zero for existing files.

1.2.2 Sequence of words is (1, 1), (2, 1),... ..(50, 1), (1, 2)...(50, 2), (1, 3)....(50, 3).

1.2.3 Above words are 60 bit integers

1.3 EOF mark

2.0 Data file ID Record, Integers

Word	1	Satellite No.
	2	Station No.
	3	Analog Tape No.
	4	Data recorded, Year (eg 1970)
	5	" " , Month (1-12)
	6	" " , Day
	7	Group No.
	8	File Status
	9	100 × % Data Recovery
	10	100 × % comb filter
	11	Physical file count (2, 3, 4...)

Quantities in words 1-10 are obtained from the corresponding record of the Goddard 3DME tape, translated to 60 bit integers.

2.1 Data Records

486 word physical records of six 81 word logical records each. Each logical record contains one 5.12 sec telemetry sequence. The last record of a data file will be filled with zeros if it contains less than 6 telemetry sequences.

2.1.1 Structure of data record

Phys Rec. (1-486)	Logical Rec. (1-81, 1-6)	Contents		Format
1+81 × (i-1)	1, i	FOC4, FOC5	Calibrated Log_{10}(flux) (Except East detector which is telemetry volts)	"Packed" (see 2.1.2)
2+81 × (i-1)	2, i	FOC6, FOC7		
3+ etc	3, i	FOC8, FOC9		"
⋮	⋮			
etc	12, i	FOC14, FOC15		"
etc	13, i	FIC4, FIC5		"
⋮	⋮			
etc	24, i	FIC14, FIC15		"
⋮	⋮			
etc	72, i	F14C14, F14C15		"
"	73, i	Day of year		Integer
"	74, i	Milliseconds of day		"
"	75, i	Sequence counter		"
"	76, i	Digital counter (3DME)		"
"	77, i	Goddard Sequence Flag		"
"	78, i	Mode		"
"	79, i	Bx	Magnetometer (<u>ATS-E Magnetic Field Monitor Instrumentation</u> T.L. Skillman, Jan. 1970 Goddard document X-645-70-54	CDC Foating
"	80, i	By		"
81+81(i-1)	81, i	Bz		
1 + 81i	(1, i+1)			
⋮	⋮			
486	(81, 6)			

i = 1 to 6

2.1.2 Packed format

Each 60 bit word (1,i) through (72,i) contains the following.

60 – 49	48 – 37	36 – 35	34 – 33	32 – 31	30 – 19	18 – 7	6 – 5	4 – 3	2 – 1
S: Exponent	Characteristic	L	M	N	S: Exponent	Characteristic	L	M	N

30 most significant bits contain the first word (chronologically) and its identifying codes

30 least significant bits contain the second word (chronologically) and its identifying codes

2.1.2.1 The sign, exponent and characteristic are in CDC 6600 floating point form with characteristics truncated to 12 bits.

2.1.2.2 L, regarded as a 2 bit integer

L = 1, North detector
= 2, South detector
= 3, East detector

2.1.2.3 M, regarded as a 2 bit integer

M = 0, (Current)
= 1, Energy range 1
= 2, " " 2
= 3, " " 3

2.1.2.4 N, regarded as a 2 bit integer

N = 1, Electrons
= 2, Protons
= 3, Current

2.1.2.5	L	M	N	LMN as single octal integer
N0	01	00	11	23
N1E	01	01	01	25
N2E	01	10	01	31
N3E	01	11	01	35
N1P	01	01	10	26
N2P	01	10	10	32
N3P	01	11	10	36
S0	10	00	11	43
S1E	10	01	01	45
S2E	10	10	01	51
S3E	10	11	01	55
S1P	10	01	10	46
S2P	10	10	10	52
S3P	10	11	10	56
E0	11	00	11	63
E1E	11	01	01	65
E2E	11	10	01	71
E3E	11	11	01	75
E1P	11	01	10	66
E2P	11	10	10	72
E3P	11	11	10	76

2.1.2.6 Calibration of Data on Intermediate Tape

Telemetry Volts	Electrons N1E	S1E	N2E	S2E	N3E	S3E
0.0	3.42	3.05	2.16	2.58	1.39	1.50
0.25	3.61	3.25	2.40	2.80	1.66	1.69
0.50	3.80	3.45	2.64	3.02	1.93	1.88
0.75	3.97	3.68	2.86	3.20	2.16	2.07
1.00	4.15	3.90	3.09	3.39	2.39	2.26
1.25	4.31	4.11	3.31	3.60	2.59	2.47
1.50	4.48	4.33	3.52	3.82	2.79	2.67
1.75	4.65	4.54	3.76	4.04	3.01	2.86
2.00	4.81	4.75	4.00	4.25	3.23	3.05
2.25	4.98	4.94	4.22	4.43	3.43	3.24
2.50	5.14	5.13	4.44	4.60	3.63	3.43
2.75	5.29	5.31	4.62	4.79	3.81	3.61
3.00	5.45	5.49	4.80	4.97	3.99	3.78
3.25	5.60	5.65	4.98	5.14	4.15	3.94
3.50	5.75	5.81	5.16	5.32	4.32	4.11
3.75	5.90	5.98	5.34	5.49	4.49	4.25
4.00	6.04	6.14	5.52	5.67	4.66	4.39
4.25	6.19	6.30	5.70	5.86	4.84	4.55
4.50	6.34	6.45	5.88	6.05	5.02	4.71
4.75	6.49	6.61	6.08	6.22	5.18	4.86
5.00	6.64	6.77	6.27	6.39	5.34	5.02

Units, Electrons: $\mathrm{Log}_{10}\ (\mathrm{cm}^{-2}\mathrm{sec}^{-1}\mathrm{ster}^{-1}\mathrm{kV}^{-1})$

2.1.2.7 Calibration of Data on Intermediate Tape

Telemetry Volts	Current		Protons					
	N0	S0	N1P	S1P	N2P	S2P	N3P	S3P
0.0	5.32	5.65	3.02	2.66	1.64	2.23	2.32	2.04
0.25	6.12	6.30	3.21	2.86	1.88	2.45	2.59	2.22
0.50	6.92	6.95	3.40	3.05	2.11	2.67	2.86	2.41
0.75	7.49	7.25	3.58	3.28	2.34	2.86	3.09	2.60
1.00	8.06	7.54	3.75	3.50	2.57	3.04	3.32	2.80
1.25	8.53	7.79	3.92	3.71	2.78	3.26	3.52	3.00
1.50	8.99	8.03	4.08	3.93	3.00	3.47	3.72	3.20
1.75	9.40	8.30	4.25	4.14	3.24	3.69	3.94	3.39
2.00	9.81	8.57	4.41	4.36	3.48	3.91	4.16	3.58
2.25	10.1	8.86	4.58	4.54	3.70	4.08	4.36	3.77
2.50	10.5	9.14	4.74	4.73	3.92	4.25	4.56	3.97
2.75	10.8	9.40	4.90	4.91	4.10	4.44	4.74	4.14
3.00	11.1	9.65	5.05	5.10	4.28	4.63	4.92	4.31
3.25	11.3	9.90	5.20	5.26	4.46	4.80	5.08	4.47
3.50	11.6	10.1	4.35	5.42	4.64	4.97	5.25	4.64
3.75	11.7	10.4	5.50	5.58	4.82	5.15	5.42	4.78
4.00	11.9	10.6	5.64	5.74	5.00	5.33	5.59	4.93
4.25	12.0	10.8	5.79	5.90	5.18	5.52	5.77	5.08
4.50	12.1	11.0	5.94	6.05	5.36	5.71	5.95	5.24
4.75	12.1	11.1	6.09	6.21	5.55	5.88	6.11	5.39
5.00	12.1	11.3	6.24	6.38	5.75	6.04	6.27	5.55

Units, Current: Log_{10} (kV cm^{-2} sec^{-1} ster^{-1})

Protons: Log_{10} (cm^{-2} sec^{-1} ster^{-1} keV^{-1})

2.1.2.8 East data is in telemetry volts.

2.1.2.9 Times of analog data

The times given for each sequence, in words (73,i) = day of year, (74,i) = milliseconds of day, are the same as those on the Goddard 3DME tapes.

The following formula yields the time of each datum (analog)

$$t = t_o + 0.32F + 0.02C + \varepsilon$$

where t_o = time of FOCO

F = Frame number = 0, 1, 2, 4, 5, 6, 8, 9, 10, 12, 13, 14 (Note: 3, 7, 11 missing)

C = Channel number = 4 through 15

The order of words (1,i) to (72,i) is chronological.

ε is believed to be zero but may more correctly be a signed few milliseconds.

2.1.3 Magnetometer. Units are gammas. By is 68 less here than on Goddard 3DME tapes.

2.2 <u>EOF mark at the end of each file.</u> There are usually about 24 files per tape, more if data has been merged from several Goddard tapes. Each file on the intermediate tape will be a complete or truncated Goddard file but always starts with the I.D. information record of the originating Goddard 3DME tape file.

3.0 <u>EOF Mark (Empty File)</u>

4.0 There is no housekeeping data on the intermediate tapes, nor is calibration data specially processed. Calibration sequences are present however and are formally (insofar as tape structure is concerned) similar to data sequences.

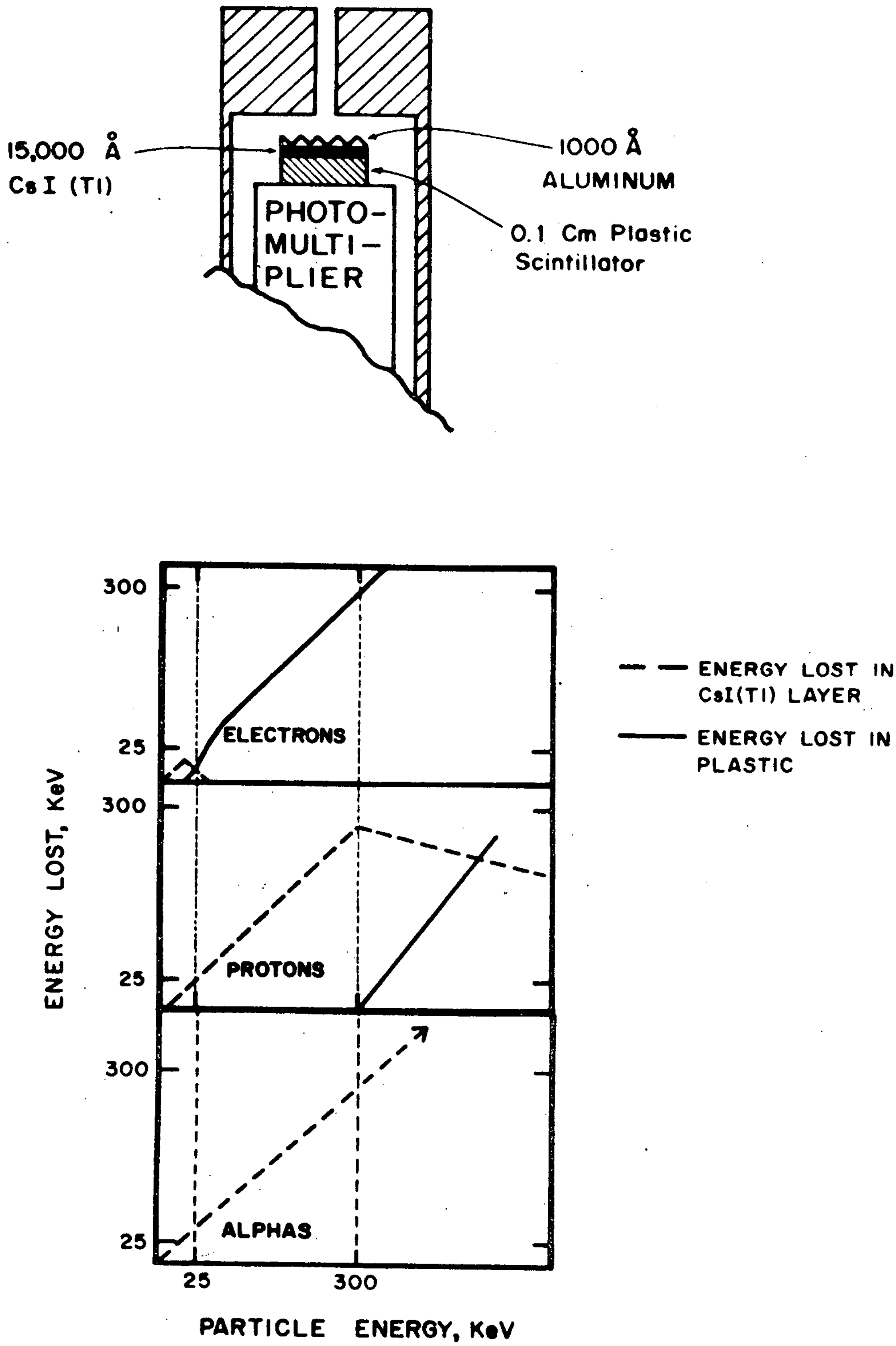
15,000 Å
CsI (Tl)
1000 Å
ALUMINUM
0.1 Cm Plastic
Scintillator
PHOTO-
MULTI-
PLIER
ENERGY LOST, KeV
300
25
ELECTRONS
PROTONS
ALPHAS
25
300
PARTICLE ENERGY, KeV
ENERGY LOST IN
CsI(Tl) LAYER
ENERGY LOST IN
PLASTIC

Figure 1

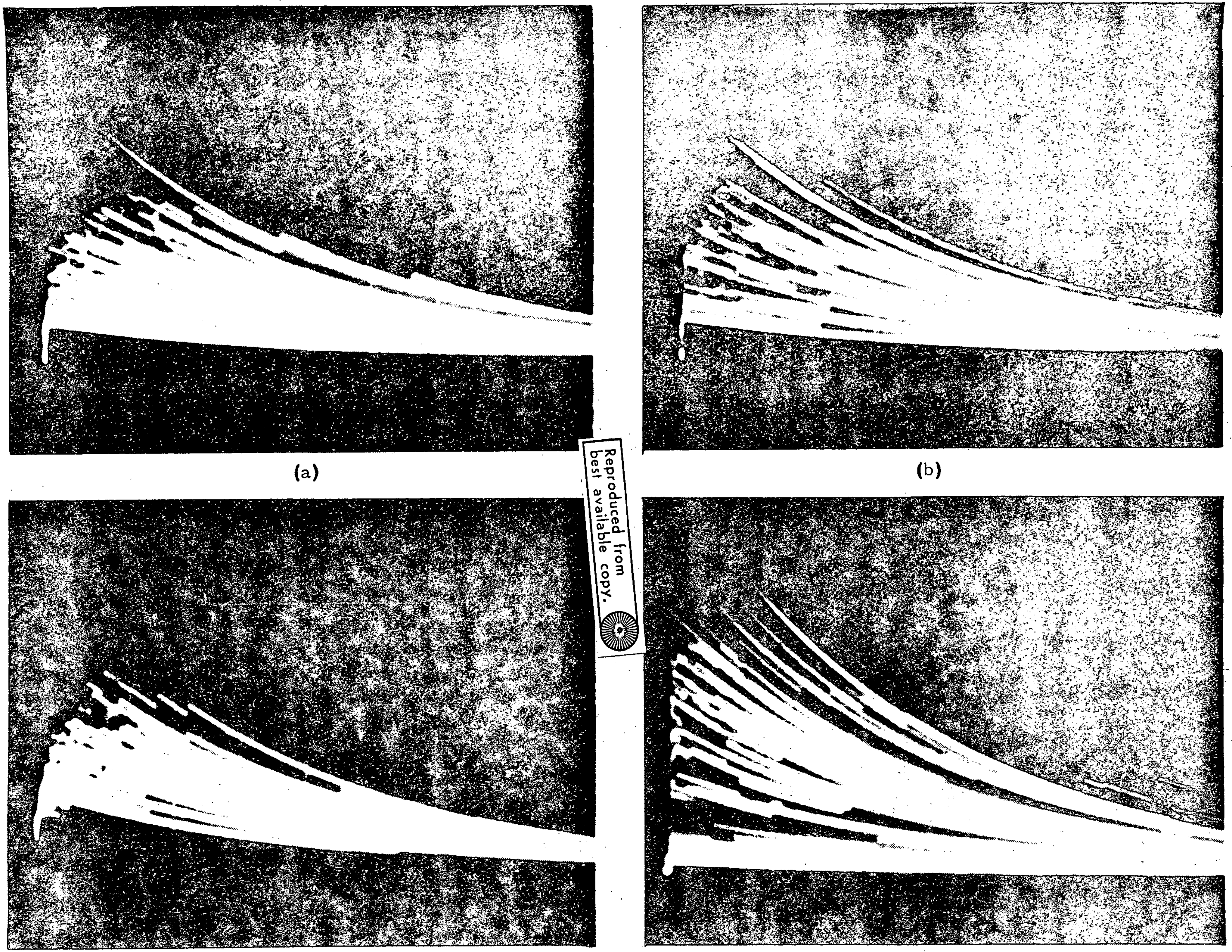

(a) (b) (c) (d)

Figure 2

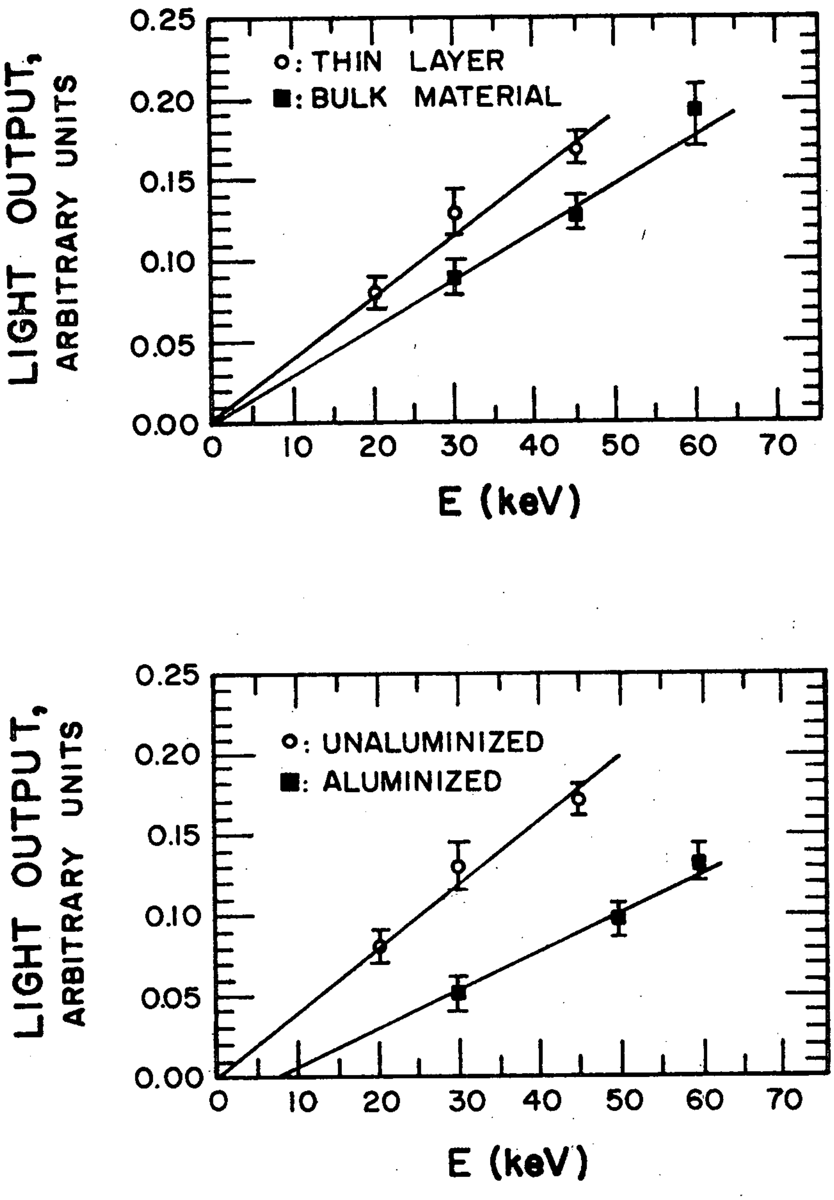
LIGHT OUTPUT, ARBITRARY UNITS
o: THIN LAYER
■: BULK MATERIAL
E (keV)
LIGHT OUTPUT, ARBITRARY UNITS
o: UNALUMINIZED
■: ALUMINIZED
E (keV)

Figure 3

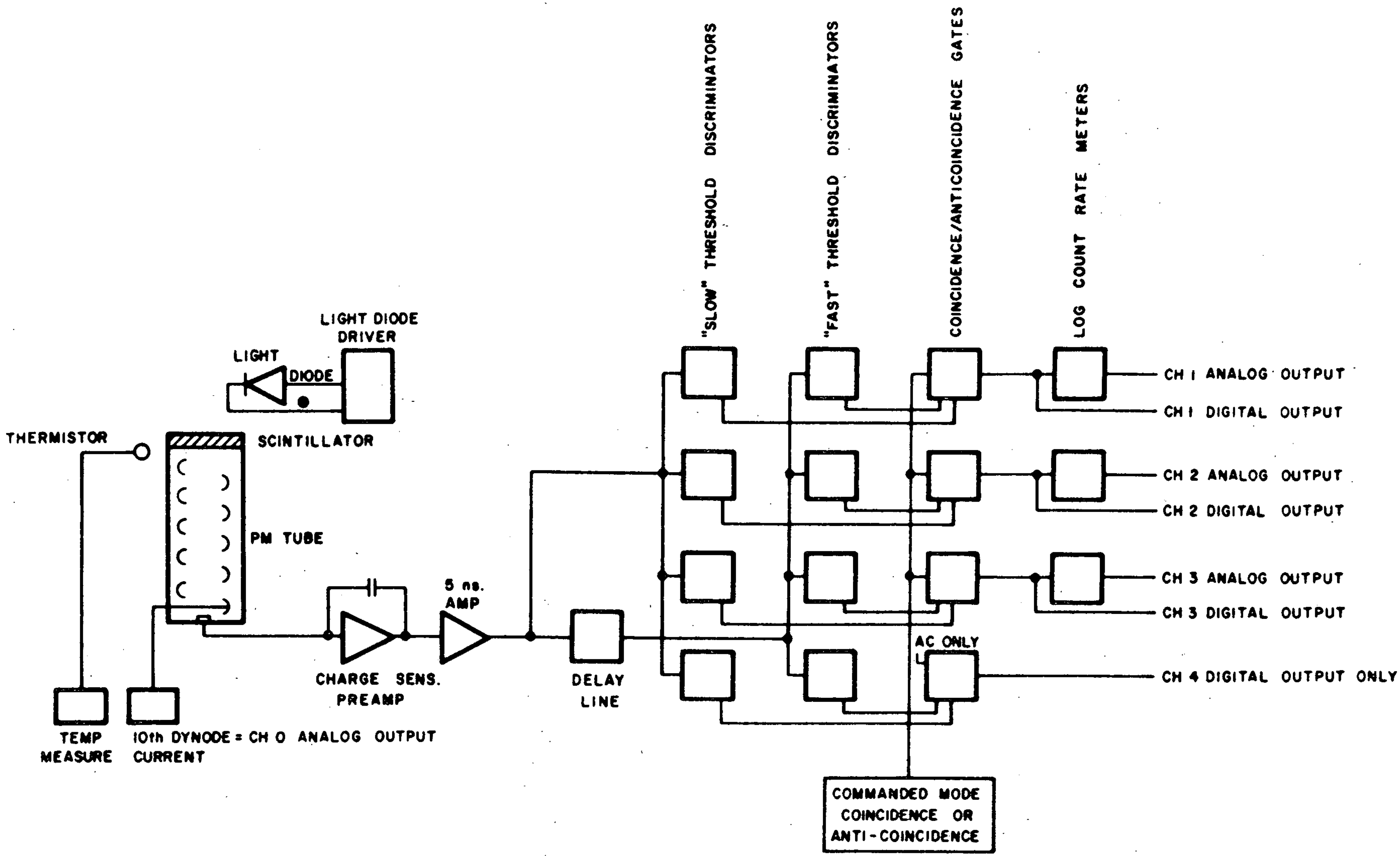

ATS-5 3DME SYSTEM DIAGRAM (ONE DETECTOR)
EXCLUDING POWER SUPPLY AND LOGIC

Figure 4

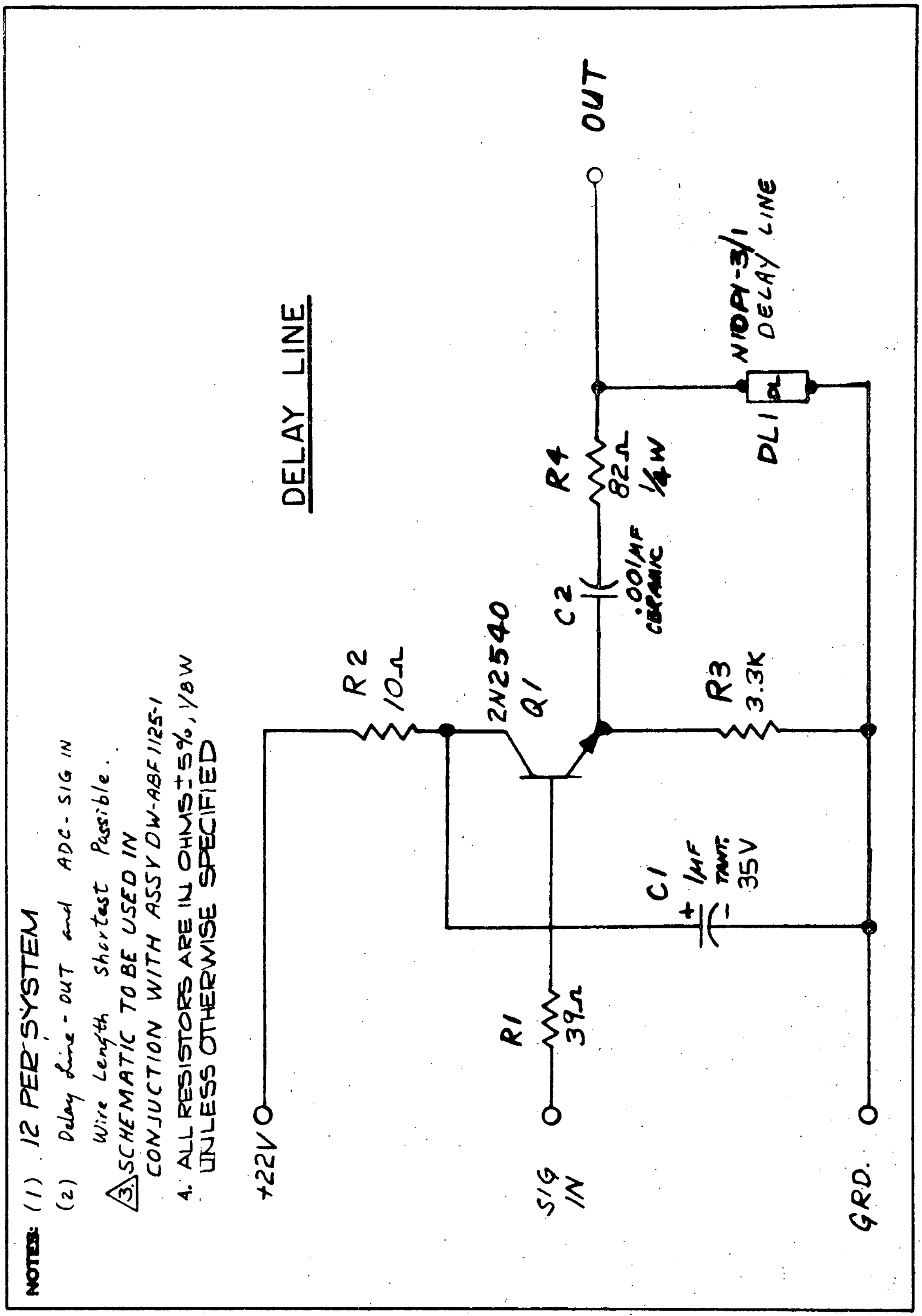
NOTES: (1) 12 PER SYSTEM
(2) Delay Line - OUT and ADC - SIG IN
Wire Length Shortest Possible.
3. SCHEMATIC TO BE USED IN CONJUCTION WITH ASSY DW-ABF1125-1
4. ALL RESISTORS ARE IN OHMS ±5%, 1/8W UNLESS OTHERWISE SPECIFIED
DELAY LINE
+22V
SIG IN
GRD.
R1
39Ω
C1
1MF
TANT.
35V
R2
10Ω
2N2540
Q1
R3
3.3K
C2
.001MF
CERAMIC
R4
82Ω
1/4W
DL1
N10P1-3/1
DELAY LINE
OUT

Figure 5

THRESHOLD DISCRIMINATOR

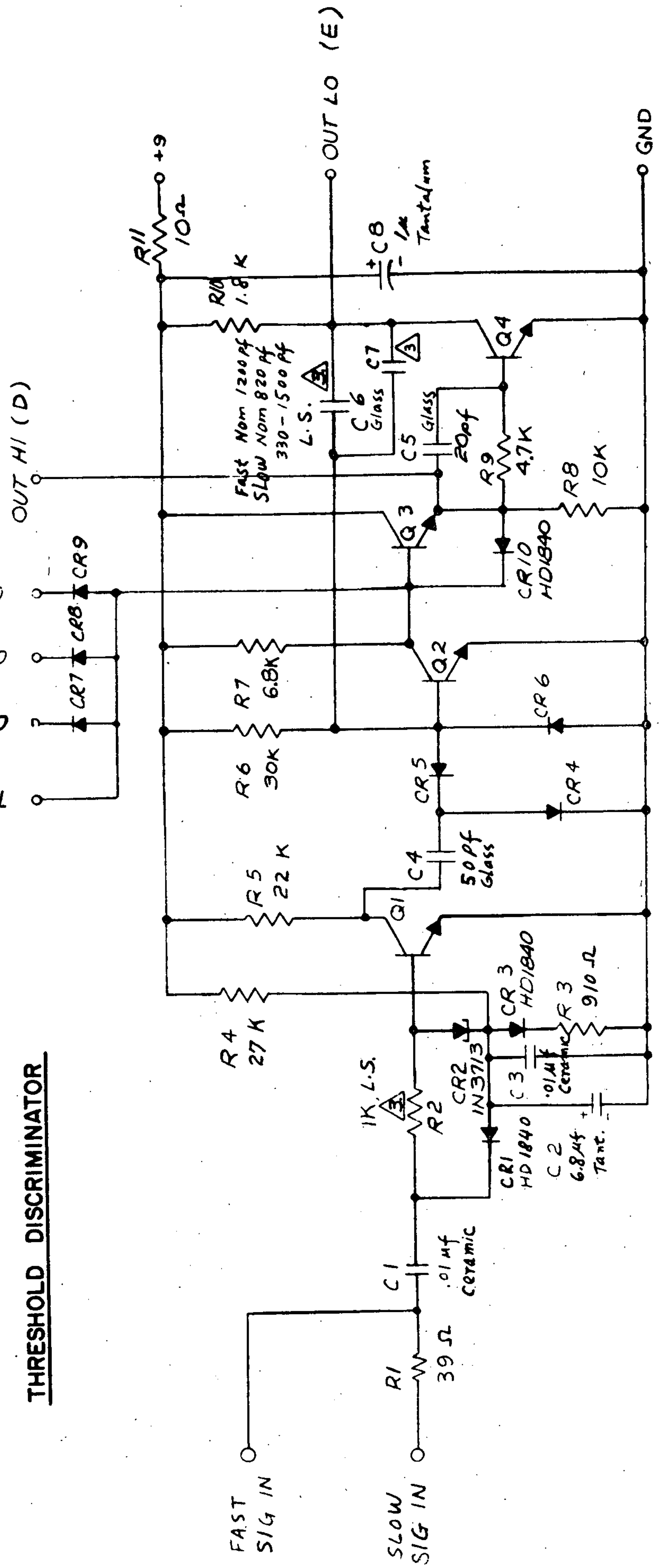

Figure 6 .

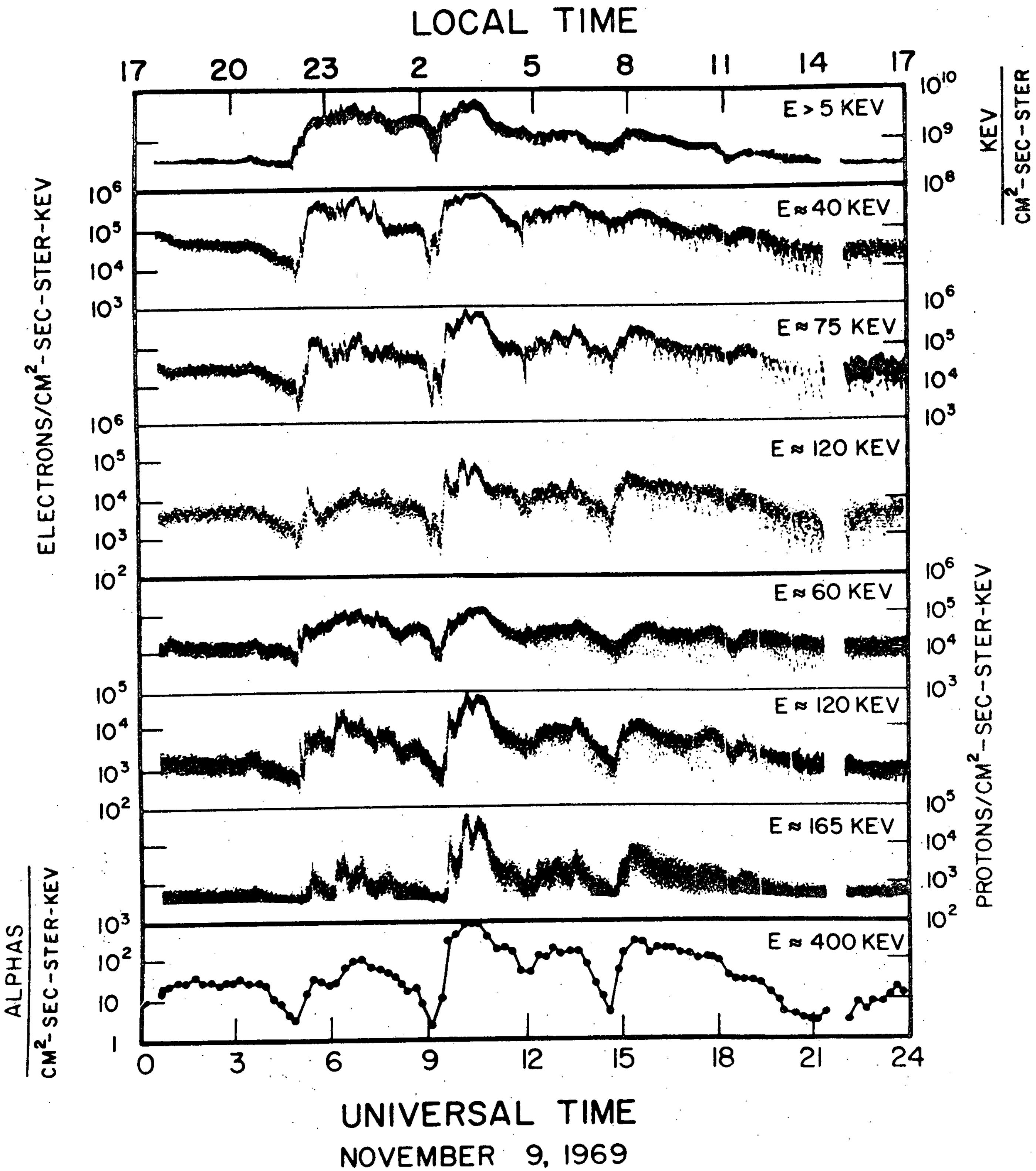
LOCAL TIME
17
20
23
2
5
8
11
14
17
E > 5 KEV
E ≈ 40 KEV
E ≈ 75 KEV
E ≈ 120 KEV
E ≈ 60 KEV
E ≈ 120 KEV
E ≈ 165 KEV
E ≈ 400 KEV
ELECTRONS/CM²-SEC-STER-KEV
PROTONS/CM²-SEC-STER-KEV
KEV / CM²-SEC-STER
ALPHAS / CM²-SEC-STER-KEV
0
3
6
9
12
15
18
21
24
UNIVERSAL TIME
NOVEMBER 9, 1969

Figure 7

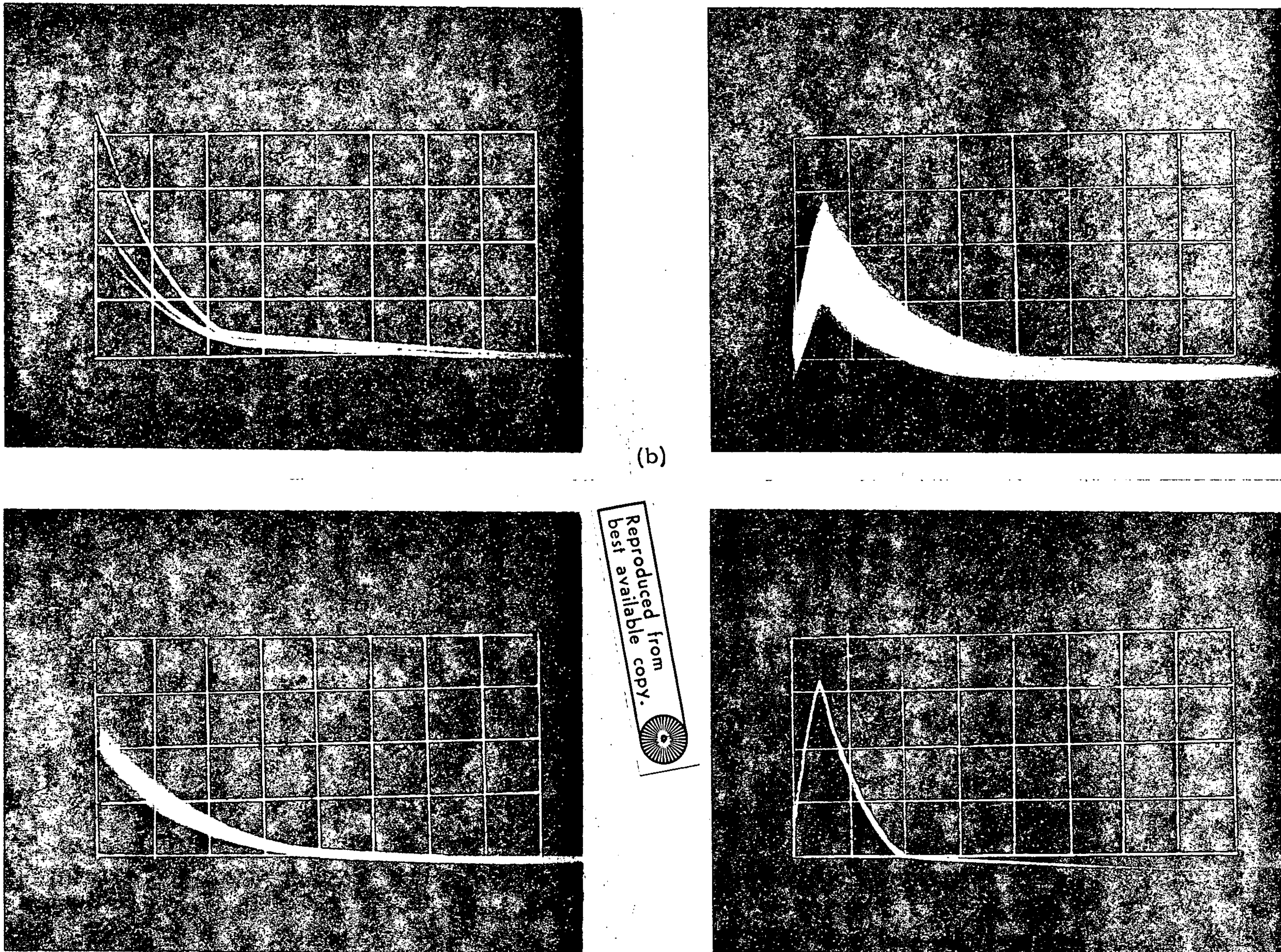

(a) (b) (c) (d)

Figure 8

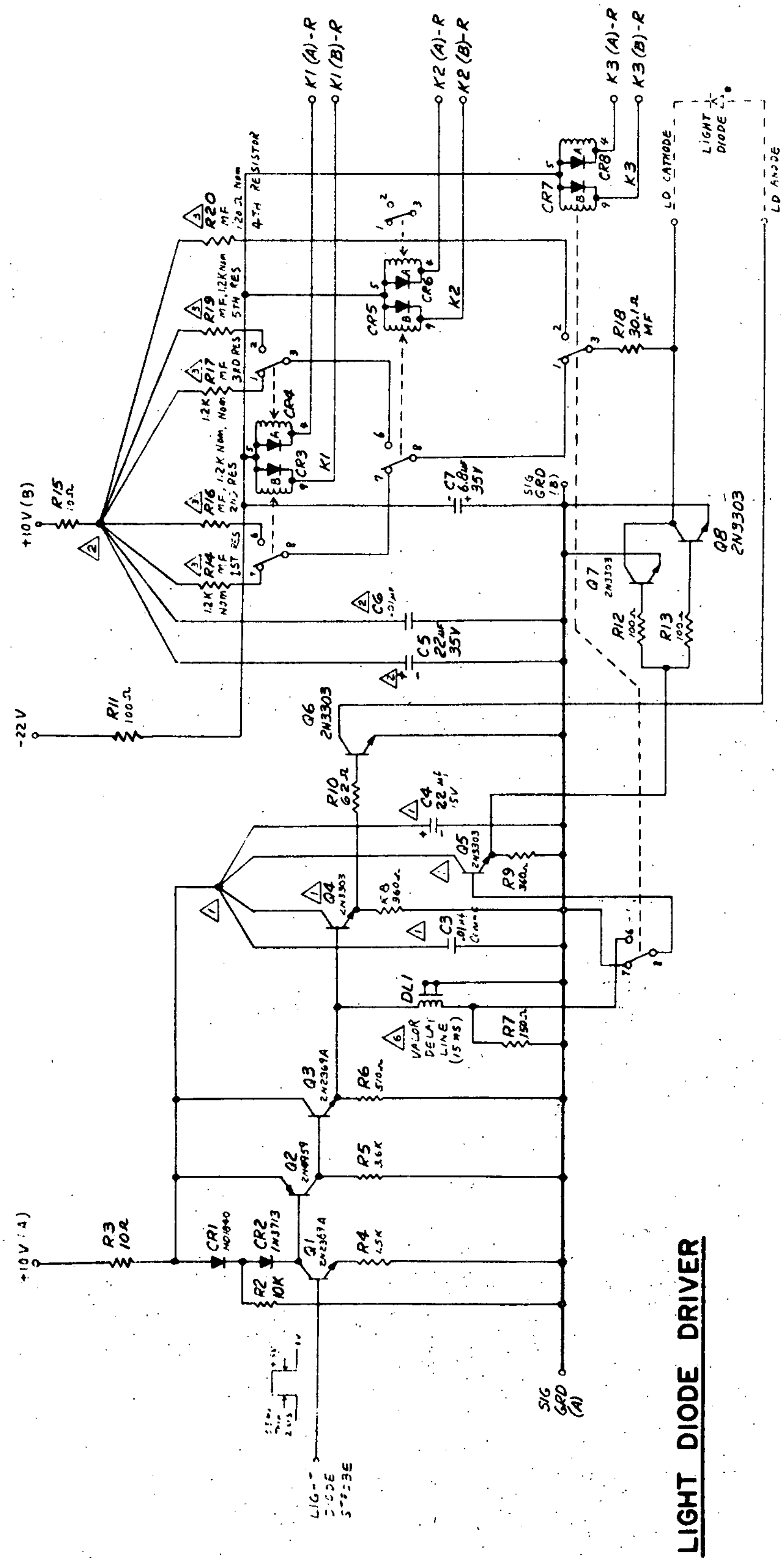

LIGHT DIODE DRIVER

Figure 9

IV. ATS-5 BIBLIOGRAPHY

1. Mozer, F.S., F.H. Bogott and C.W. Bates, Development of a double-layered scintillator for separating and detecting low energy protons and electrons, IEEE Trans. Nucl. Sci., NS-15, 144, 1968

2. Bogott, F., Magnetopause properties inferred from energetic particle measurements on ATS-5, Trans. Am. Geophys. Union, 51, 390, 1970

3. Bogott, F. and F.S. Mozer, Electron and proton pitch angle distributions measured on ATS-5, Trans. Am. Geophys. Union, 51, 806, 1970

4. Mozer, F.S. and F.H. Bogott, Energetic particle measurements on the ATS-5 synchronous satellite, Trans. Am. Geophys. Union, 51, 390, 1970

5. Bogott, F. and F.S. Mozer, Magnetopause electric field inferred from energetic particle measurements on ATS-5, J. Geophys. Res., 76, 892-899, 1971

6. Bogott, F., Energetic particle measurements at the synchronous orbit, PhD Thesis, Physics Department, University of California, Berkeley, February 1971

7. Mozer, F.S., Power spectra of the magnetospheric electric field, J. Geophys. Res., 76, 3651-3667, 1971

8. Mozer, F.S. and F.H. Bogott, Equatorial proton and electron angular distributions in the loss cone and at large angles, J. Geophys. Res., 76, 6790-6805, 1971

9. Mozer, F.S., Origin and effects of electric fields during isolated magnetospheric substorms, J. Geophys. Res., 76, 7595-7608, 1971

10. Mozer, F.S. and F.H. Bogott, Photoelectron emission from Io as the cause of enhancements of the Jovian decametric radiation, Astrophys. J., April, 1972 (in press)

11. Mozer, F.S., F.H. Bogott and N. Brice, Triggered acceleration of 50 kilovolt protons and electrons, J. Geophys. Res., submitted

12. Mozer, F.S., Particle flux limits in the synchronous orbit, J. Geophys. Res., submitted

13. Mozer, F.S., F.H. Bogott and B. Tsurutani, Relations between ionospheric electric fields and energetic trapped and precipitating electrons, J. Geophys. Res., submitted

14. Tsurutani, B. and F.H. Bogott, The onset of magnetospheric substorms, J. Geophys. Res., submitted

15. Mozer, F.S., On the relationship between DP-1, DP-2, the growth and expansion phases of substorms, and ionospheric electric fields, J. Geophys. Res., (submitted)